

Article

Analog Electromagnetic Black Holes Made of Water

Igor I. Smolyaninov

Saltenna LLC, 1751 Pinnacle Drive, Suite 600, McLean, VA 22102-4903, USA; igor.smolyaninov@saltenna.com

How To Cite: Smolyaninov, I.I. Analog Electromagnetic Black Holes Made of Water. *International Journal of Gravitation and Theoretical Physics* **2025**, *1*(1), 7. <https://doi.org/10.53941/ijgtp.2025.100007>

Received: 13 July 2025

Revised: 18 September 2025

Accepted: 22 September 2025

Published: 24 September 2025

Abstract: A novel analog black hole model is introduced, which is based on the divergent dielectric permittivity of water in the radio frequency range. An interesting aspect of this system is the possibility to study the appearance of surface electromagnetic modes in such an analog black hole model. The gravity-capillary waves on the water surface, which act as analogs of spacetime fluctuations, lead to appearance of gradient surface electromagnetic waves at the emulated horizon. Such models become especially interesting in the case of extreme Reissner-Nordstrom black holes which are shown to behave as spherical waveguide resonators, in which photons and gravitons acquire effective mass. Optical and gravitational wave lasing may be expected in such situations based on the analogy with optical whispering gallery mode lasers made of water droplets.

Keywords: analog black hole; water; extreme Reissner-Nordstrom black hole

1. Introduction

Recent advances in electromagnetic metamaterials and transformation optics brought renewed attention to the well-known analogy between many electromagnetic and general relativity situations [1,2], in which empty but curved spacetime manifolds may appear as effective dielectric media. Indeed, in an empty but possibly curved spacetime, the effective dielectric permittivity and magnetic permeability are [1,2]:

$$\varepsilon^{ij} = \mu^{ij} = -\frac{\sqrt{-g}}{g_{00}} g^{ij} \quad (1)$$

resulting in several suggestions to emulate black holes using non-trivial electromagnetic materials exhibiting divergent ε and/or μ behaviour in some range of physical parameters, such as electromagnetic frequency, temperature, pressure, etc. [3–5]. For example, the effective radius-dependent electromagnetic parameters of a Reissner-Nordstrom black hole may be found as

$$\varepsilon = \mu = \frac{1}{\sqrt{1 - \frac{2M}{r} + \frac{Q^2}{r^2}}} \quad (2)$$

where M and Q are the black hole mass and charge, respectively [6]. As may be observed from Equation (2), the effective dielectric permittivity and magnetic permeability of a black hole, and its effective refractive index diverge at the horizon, and they become very large complex numbers inside a black hole, if one to believe the analytic continuations of Equations (2) and (3) beyond the horizon. Not surprisingly, various multiferroic materials exhibiting very large ε and/or μ were suggested in the past as appropriate materials to build an electromagnetic black hole model in a laboratory [3,6]. On the other hand, on the gravity theory side, it was demonstrated that coupling an antisymmetric tensor field to the electromagnetic field in a dyonic Reissner-Nordstrom-AdS black hole background results in a holographic model for the paramagnetism/ferromagnetism phase transition [7]. Such a convergence of properties of laboratory and field theoretical black hole models illustrates the considerable power and usefulness of the analogue gravity approach.



Copyright: © 2025 by the authors. This is an open access article under the terms and conditions of the Creative Commons Attribution (CC BY) license (<https://creativecommons.org/licenses/by/4.0/>).

Publisher's Note: Scilight stays neutral with regard to jurisdictional claims in published maps and institutional affiliations.

$$n = \sqrt{\varepsilon\mu} = \frac{1}{\sqrt{1 - \frac{2M}{r} + \frac{Q^2}{r^2}}} \quad (3)$$

Unfortunately, various metamaterial approaches to analogue gravity also suffer common difficulties due to the apparent lack of natural and artificial materials exhibiting considerable magnetic response. The typical metamaterial black hole models introduced so far limit themselves to the case of $\mu = 1$, and mimic the black hole properties based on the divergent behaviour of the frequency-dependent refractive index (Equation (3)) of the metamaterial structure—see for example refs. [3,5]. We are going to follow the same approach in our discussion below.

In this paper we are going to look at another example of an electromagnetic material exhibiting divergent dielectric properties. Unlike some sophisticated metamaterial-based models introduced in the past [5], we are going to consider a black hole model made of ordinary water. As discussed in [8], the frequency dependent dielectric permittivity of water in the radio frequency range may be calculated as

$$\varepsilon_w = \varepsilon_\infty + \frac{\varepsilon_{stat} - \varepsilon_\infty}{1 + i\omega\tau} - \frac{\sigma}{i\omega\varepsilon_0} \quad (4)$$

where $\varepsilon_\infty = 5.1$, $\varepsilon_{stat} = 79.2$, $\tau = 8.72$ ps, σ is salinity-defined conductivity, and ε_0 is vacuum permittivity. The real ε' and imaginary ε'' parts of water dielectric permittivity are plotted in Figure 1 for several levels of water salinity, corresponding to the typical conductivities of pure water, fresh water, pool water, and sea water, respectively. Figure 1 illustrates a very fast divergence of ε'' in the $\omega \rightarrow 0$ limit, leading to extremely large magnitudes of the refractive index of water in the low frequency range:

$$n = \frac{1+i}{\sqrt{2}} \left(\frac{\sigma}{\varepsilon_0\omega} \right)^{1/2} \rightarrow \infty \quad (5)$$

(for the details of complex frequency-dependent dielectric permittivity formalism a reader may address ref. [9]). If we understand an electromagnetic black hole as a spherical object having a very large refractive index, using a water droplet is one of the best and simplest ways to create such an object. In the next section we will demonstrate that water droplets may indeed be used to illustrate and emulate some very interesting black hole properties.

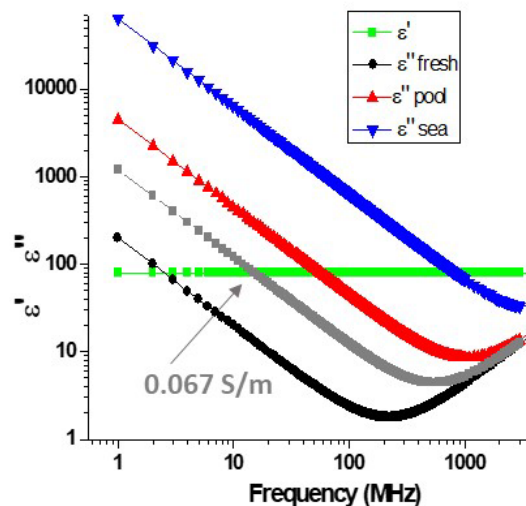


Figure 1. Plots of the magnitudes of real ε' and imaginary ε'' parts of water permittivity calculated at different levels of water salinity. The real part ε' of the dielectric permittivity of water is shown by green data points. The frequency-dependent imaginary part ε'' of water dielectric permittivity are shown by black, grey, red and blue data points for the typical levels of electric conductivity in pure water (0.011 S/m), fresh drinking water (0.067 S/m), pool water (0.25 S/m) and seawater (3.5 S/m), respectively.

2. Gradient Surface Electromagnetic Waves Near a Water-Based Analogue Black Hole

Potential existence of surface electromagnetic modes near a Schwarzschild back hole horizon has been analyzed in a recent paper [10], which concluded that such surface wave solutions may appear at the horizon when

quantum gravity effects are taken into account. This conclusion is important because the presence of surface electromagnetic modes should lead to such interesting effects as optical second harmonic generation by a Schwarzschild back hole [10], which may provide us with a rare observational tool to study quantum gravity.

For the sake of further discussion, let us recall the consideration of gradient surface electromagnetic waves in a generic gradient medium scenario in which both ε and μ vary as a function of z coordinate [11]. This consideration applies to numerous macroscopic electrodynamics scenarios, and it may be also applied to some gravity theory situations [10], assuming the coordinate dependencies of ε and μ described by Equations (1) and (2). As discussed in detail in [11], the wave equation for transverse magnetic (TM) modes (these are the electromagnetic field modes in which the magnetic field is always perpendicular to the direction of propagation) inside such a gradient medium may be written as an effective one-dimensional Schrodinger equations

$$-\frac{\partial^2 \psi}{\partial z^2} + \left(-\frac{\varepsilon(z)\mu(z)\omega^2}{c^2} - \frac{1}{2} \frac{\partial^2 \varepsilon}{\partial z^2} + \frac{3}{4} \frac{(\partial \varepsilon / \partial z)^2}{\varepsilon^2} \right) \psi = -\frac{\partial^2 \psi}{\partial z^2} + V(z)\psi = -k^2 \psi \quad (6)$$

where k is the photon wave vector in the xy plane, $V(z)$ is an effective potential, and the effective wave function is introduced as $\psi = \varepsilon^{1/2} E_z$, where E_z is z -component of the electric field. In the case of a Schwarzschild back hole the effective potential near horizon was obtained in [9] as

$$V \approx -\frac{2\omega^2 M}{c^2 \rho} - \frac{3}{16\rho^2} \quad (7)$$

where it is assumed that $r = 2M + \rho$ and $\rho \ll 2M$, so that a Schwarzschild black hole near the horizon may be described as a planar gradient medium in which the coordinate ρ may be identified as coordinate z in Equation (6). In the absence of potential cutoff, which might be introduced at small ρ by hypothetic quantum gravity effects, there is no finite ground state in this potential, so that all electromagnetic modes fall into the horizon. On the other hand, it was noted in [10] that any potential well that is weaker than $1/\rho^2$ exhibits a finite ground state. Therefore, the emergence of a cutoff for any reason in the divergent $1/\rho^2$ behavior of the potential $V(\rho)$ near a black hole event horizon (for example, due to the existence of quantum gravitational minimum length l_{min} of the order of the Planck scale) leads to the emergence of a well-defined ground eigenstate among the wave functions described by Equation (6) [10].

Let us demonstrate how this effect may be emulated by a water-based black hole model, in which an effective horizon is located at the water surface. First, let us recall the classic derivation of surface electromagnetic wave solutions near an interface between two media. In a classic derivation the interface is considered to be a step-like infinitely sharp transition (leading to a strongly divergent $V(z)$ at the interface—see Equation (6)), and the surface wave solution is obtained based on matching the boundary conditions for electric and magnetic fields at the interface. The resulting surface wave dispersion relation is:

$$k = \frac{\omega}{c} \left(\frac{\varepsilon_1 \varepsilon_2}{\varepsilon_1 + \varepsilon_2} \right)^{1/2} \quad (8)$$

where ε_1 and ε_2 are the dielectric permittivities of the neighboring media [12]. If a sharp step-like interface between vacuum ($\varepsilon_1 = 1$) and a medium having a very large imaginary ε_2 is considered, which corresponds to the behavior of water in the low (radio) frequency electromagnetic field region (see Equation (4)) and the behavior of Equation (2) below the horizon, the resulting Zenneck wave solution appears to be un-physical due to the superluminal answer given by Equation (8) [13]. On the other hand, the real physical water surface is always wavy due to the gravity-capillary waves (see Figure 2b) which are always present on the water surface, and this waviness leads to pushing the surface electromagnetic wave solution into the physical domain [11]. The gravity-capillary waves play the role of spacetime fluctuations, removing the divergencies in $V(z)$ and leading to a well-defined ground state in the surface electromagnetic wave spectrum of the water-air interface.

In fact, a basic analysis of Equation (6) indicates quite a generic appearance of surface electromagnetic wave solutions for a general gradual interface between two media. Indeed, if we consider a generic z -dependent dielectric permittivity profile near an interface

$$\varepsilon(z) = a(z)e^{i\delta(z)} \quad (9)$$

where $a(z)$ is the absolute value of the dielectric constant and $\delta(z)$ is the loss angle, the effective surface potential at low frequencies is dominated by the gradient term in Equation (6), so that

$$\frac{d\varepsilon}{dz} = \frac{da}{dz} e^{i\delta} + iae^{i\delta} \frac{d\delta}{dz} = ae^{i\delta} \left(\frac{d(\ln a)}{dz} + i \frac{d\delta}{dz} \right) \approx i\varepsilon \frac{d\delta}{dz} \quad (10)$$

and

$$V(z) \approx -\frac{3}{4} \left(\frac{d\delta}{dz} \right)^2 \quad (11)$$

A shallow potential well develops near an interface, which supports a surface electromagnetic state. This potential well behaves as an effective surface waveguide. This surface waveguide may be used by divers to achieve surface wave-based radio communication underwater [14], as illustrated in Figure 2. In the next section we will demonstrate that the surface waveguide analogy appears to be quite literal in the case of an extreme Reissner-Nordstrom black hole.

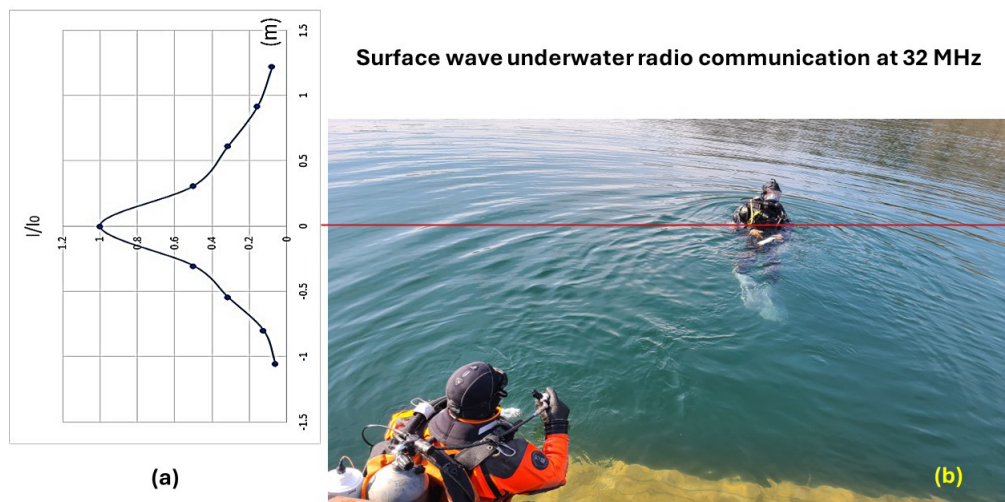


Figure 2. (a) Experimentally measured radio frequency electromagnetic field intensity in the direction perpendicular to the water-air interface clearly indicates excitation of a surface electromagnetic wave. (b) Divers performing characterization of the surface wave-based underwater radio communication system operating at 32 MHz. Gravity-capillary waves are always present on the water surface.

3. Extreme Reissner-Nordstrom Black Hole as a Spherical Waveguide Resonator

Let us consider the extreme Reissner-Nordstrom metric

$$ds^2 = \left(\frac{r-M}{r} \right)^2 c^2 dt^2 - \left(\frac{r}{r-M} \right)^2 dr^2 - r^2 d\theta^2 - r^2 \sin^2 \theta d\phi^2 \quad (12)$$

Introducing coordinate transformation

$$r = M \left(1 + e^{\frac{\tilde{z}}{M}} \right) \quad (13)$$

and assuming $\sin \theta = 1$ leads to

$$ds^2 = \frac{e^{\frac{2\tilde{z}}{M}}}{\left(1 + e^{\frac{\tilde{z}}{M}} \right)^2} c^2 dt^2 - \left(1 + e^{\frac{\tilde{z}}{M}} \right)^2 \left(d\tilde{z}^2 - M^2 d\theta^2 - M^2 d\phi^2 \right) \quad (14)$$

which results in a Cartesian spatial metric in the vicinity of the extreme Reissner-Nordstrom black hole if $Md\theta$ and $Md\phi$ are identified as dx and dy , respectively. Application of Equation (1) to the spacetime metric (14) leads to an

expression for the equivalent dielectric permittivity and magnetic permeability of an extreme Reissner-Nordstrom black hole:

$$\varepsilon = \mu = 1 + e^{\frac{z}{M}} = \frac{r}{|r - M|} \quad (15)$$

It is clear that these equivalent ε and μ parameters describe a spherical waveguide. Indeed, in this waveguide $\varepsilon = \mu = 1$ at $r = \infty$ and $r = M/2$, and $\varepsilon = \mu \rightarrow \infty$ at $r = M$. The so obtained effective parameters $\varepsilon(z) = \mu(z)$ (described by Equation (15)) may be substituted into Equation (6) to obtain the wave equation describing propagation of electromagnetic waves in the Reissner-Nordstrom spacetime metric (14). Based on Equation (6) in which ε and μ are substituted from Equation (15), the wave equation for surface electromagnetic mode propagation in this waveguide is

$$-\frac{\partial^2 \psi}{\partial z^2} + \left(-\frac{\left(1 + e^{\frac{z}{M}}\right)^2 \omega^2}{c^2} + \frac{1}{4M^2} \right) \psi = -k^2 \psi \quad (16)$$

This wave equation describes electromagnetic wave propagation for both transverse magnetic (TM) and transverse electric (TE) polarization states of the electromagnetic field, since in the $\varepsilon = \mu$ cases both equations coincide [15]. It is interesting to note that similar to results of [16], both photons and gravitons in this waveguide acquire an effective mass:

$$\frac{\left(1 + e^{\frac{z}{M}}\right)^2 \omega^2}{c^2} \approx k^2 + \frac{1}{4M^2} \quad (17)$$

which in conventional units equals

$$m_{\text{eff}} \approx \frac{m_{\text{pl}}^2}{4M} \quad (18)$$

The latter conclusion is not surprising since both simple geometrical constraints and various non-trivial spacetime geometries are known to induce effective photon mass in many situations. For example, it is well known that photons propagating inside various optical waveguides acquire effective mass [17]. A geometry-induced effective photon mass also arises in Kaluza-Klein theories [18] and numerous other general relativity situations [19], even though the electromagnetic field equations remain massless at the fundamental level. For example, the dispersion law of photons propagating inside an empty rectangular optical waveguide looks like dispersion law of a massive quasi-particle:

$$\frac{\omega^2}{c^2} = k_x^2 + \frac{\pi^2 I^2}{d^2} + \frac{\pi^2 J^2}{b^2} \quad (19)$$

where ω is the photon frequency, k_x is the photon wave vector in the propagation x-direction, d and b are the waveguide dimensions, and I and J are the mode numbers in the y- and z- directions, respectively. The effective inertial rest mass of the photon in the waveguide is

$$m_{\text{eff}} = \frac{\hbar \omega_{ij}}{c^2} = \frac{\hbar}{c} \left(\frac{\pi^2 I^2}{d^2} + \frac{\pi^2 J^2}{b^2} \right)^{1/2} \quad (20)$$

Note that the particle masses in Kaluza-Klein theories have exactly the same origin [18]. The particle masses are defined by the scale of the microscopic hidden (“waveguide”) dimensions.

4. Discussion: Lasers and “Grasers” Based on the Extreme Reissner-Nordstrom Black Holes

Continuing our discussion on the similarities between the water-based analog and real black holes, we must remark that surface electromagnetic “whispering gallery” modes in water droplets are often used to build lasers [20]. In these experimental configurations (see Figure 3) the water droplet surface acts as an optical resonator, the

water is doped with some dye, so that the optical energy at a different wavelength may be pumped into this resonator, and finally, the spherical symmetry of the droplet is broken at some point so that an optical laser beam may be formed emanating from this point. Therefore, it is natural to expect that the above-mentioned similarities between the near-extreme Reissner-Nordstrom black holes and the water-based spherical waveguide resonators (in which the effective horizon is located at the water surface) may result in optical and gravitational wave lasing by such black holes. While optical lasing is quite abundant in nature, the potential to observe gravitational lasers or “grasers” appears to be quite interesting. Typical “graser” proposals involve slowly spatially varying gravitational potentials acting as mirrors and using stimulated emission of gravitational radiation by relativistic neutral [21] or charged particle beams in external fields [22]. However, the expected coupling of particles and gravitational waves in such configurations is quite weak, so these proposals do not appear particularly realistic. A near-extreme Reissner-Nordstrom black hole pumped by an asymmetric stream of infalling matter appears to be a much more realistic scenario to observe the gravitational equivalent of lasing. It will be a worthy goal to continue theoretical investigation of such scenarios in more detail.

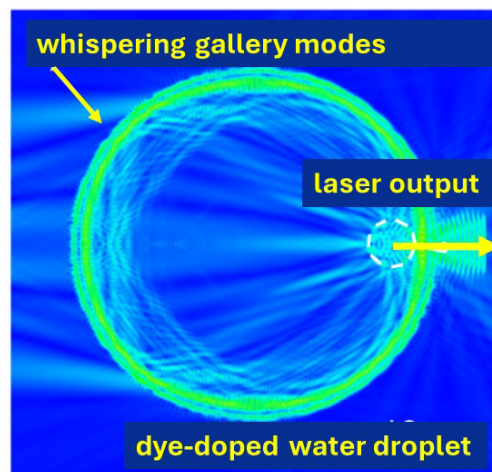


Figure 3. Schematic diagram of a water-based whispering gallery mode laser. The water droplet is doped with dye, so that it could be pumped with optical energy at a different wavelength. The droplet symmetry is broken to enable an output laser beam. A similar “graser” configuration may consist of a near-extreme Reissner-Nordstrom black hole pumped by an asymmetric stream of infalling matter.

Funding

This research received no external funding.

Institutional Review Board Statement

Not applicable.

Informed Consent Statement

Not applicable.

Data Availability Statement

No data were generated or analyzed in the presented research.

Conflicts of Interest

Given the role as Editorial Board Member, Igor I. Smolyaninov had no involvement in the peer review of this paper and had no access to information regarding its peer-review process. Full responsibility for the editorial process of this paper was delegated to another editor of the journal.

Use of AI and AI-Assisted Technologies

No AI tools were utilized for this paper.

References

1. Leonhardt; U.; Philbin, T.G. General relativity in electrical engineering. *New J. Phys.* **2006**, *8*, 247.
2. Landau; L.D.; Lifshitz, E.M. *The Classical Theory of Fields*; Pergamon Press: New York, NY, USA, 1971; Volume 2.
3. Reznik, B. Origin of the thermal radiation in a solid-state analog of a black hole. *Phys. Rev. D* **2000**, *62*, 044044.
4. Smolyaninov, I.I. Surface plasmon toy-model of a rotating black hole. *New J. Phys.* **2003**, *5*, 147.
5. Cheng; Q.; Cui; T.J.; Jiang; W.X.; et al. An electromagnetic black hole made of metamaterials. *arXiv* **2009**, arXiv:0910.2159.
6. Turimov; B.; Smolyaninov, I.I. Curved spacetime as a dispersive multiferroic medium for an electromagnetic wave: Polarization and magnetization vectors in the Schwarzschild spacetime. *Chin. J. Phys.* **2023**, *85*, 186–195.
7. Cai, R.-G.; Yang, R.-Q. Paramagnetism-ferromagnetism phase transition in a dyonic black hole. *Phys. Rev. D* **2015**, *91*, 026001.
8. Nguenouho, O.S.B.; Chevalier, A.; Potelon, B.; et al. Dielectric characterization and modelling of aqueous solutions involving sodium chloride and sucrose and application to the design of a bi-parameter RF-sensor. *Sci. Rep.* **2022**, *12*, 7209.
9. Landau, L.D.; Lifshitz, E.M. *Electrodynamics of Continuous Media*; Pergamon Press: New York, NY, USA, 1984; Volume 8.
10. Smolyaninov, I.I. Surface electromagnetic waves near a black hole event horizon and their observational consequences. *Astronomy* **2022**, *1*, 49.
11. Smolyaninov, I.I. Surface electromagnetic waves in lossy conductive media: Tutorial. *J. Opt. Soc. Am. B* **2022**, *39*, 1894.
12. Zayats, A.V.; Smolyaninov, I.I.; Maradudin, A. Nano-optics of surface plasmon-polaritons. *Phys.Rep.* **2005**, *408*, 131–314.
13. Kukushkin, A.V. On the existence and physical meaning of the Zenneck wave. *Phys. Uspekhi* **2009**, *52*, 755.
14. Smolyaninov, I.I.; Balzano, Q.; Davis, C.C.; et al. Surface wave-based underwater radio communication. *IEEE Antennas Wirel. Propag. Lett.* **2018**, *17*, 2503–2507.
15. Smolyaninov, I.I.; Balzano, Q.; Smolyaninova, V.N.; et al. Electromagnetic signal propagation through lossy media via surface electromagnetic waves. *Nanophotonics* **2024**, *13*, 1005–1015.
16. Smolyaninov, I.I. Effective photon mass in the presence of gravity gradient emulated by an electromagnetic medium. *J. Opt. Soc. Am. B* **2024**, *41*, 1901.
17. de Broglie, L. *Problemes de Propagations Guidees des Ondes Electro-Magnetiques*; Gauthier-Villars: Paris France, 1941.
18. Witten, E. Search for a realistic Kaluza-Klein theory. *Nucl. Phys. B* **1981**, *186*, 412.
19. Emelyanov, S. Effective photon mass from black-hole formation. *Nucl. Phys. B* **2017**, *919*, 110.
20. Lin, H.-B.; Huston, A.L.; Justus, B.L.; et al. Some characteristics of a droplet whispering-gallery-mode laser. *Opt. Lett.* **1986**, *11*, 614.
21. Strelkov, A.V.; Petrov, G.A.; Gagarski, A.M.; et al. Quantum states of neutrons in the Earth's gravitational field. *Nature* **2002**, *415*, 297.
22. Bessonov, E.G. Grasers based on particle accelerators and on lasers. *arXiv* **1998**, arXiv:physics/9802037.